

# Quadrupole dominance in light Cd and Sn isotopes

A. P. Zuker

Université de Strasbourg, IPHC, CNRS, UMR7178 Strasbourg, France\*

(Dated: March 13, 2021)

Shell model calculations with the neutron effective charge as single free parameter describe well the  $B(E2 : 2^+ \rightarrow 0^+)$  and  $B(E2 : 4^+ \rightarrow 2^+)$  rates for  $N \leq 64$  in the Cd and Sn isotopes. The former exhibit weak permanent deformation corroborating the prediction of a pseudo SU3 symmetry, which remains of heuristic value in the latter, though the pairing force erodes the quadrupole dominance. Calculations in  $10^7$  and  $10^{10}$ -dimensional spaces exhibit almost identical patterns: A vindication of the shell model. For  $N \geq 64$  quadrupole dominance is accentuated in the Cd isotopes and gives way to seniority dominance for the Sn isotopes.

All nuclear species are equal, but some are more equal than others. The tin isotopes deserve pride of place, because  $Z = 50$  is the most resilient of the magic numbers, because they are very numerous, and many of them stable, starting at  $A = 112$ . For these, accurate data have been available for a long time. As seen in Fig. 1 a parabola accounts very well for the  $B(E2 : 2^+ \rightarrow 0^+)$  trend, except at  $^{112-114}\text{Sn}$ .

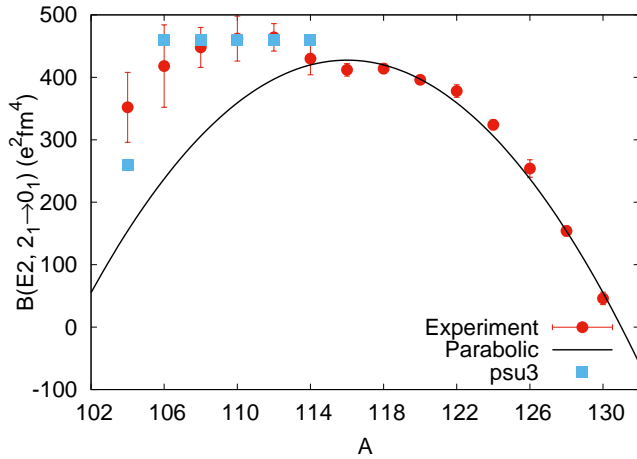


FIG. 1. The experimental  $B(E2 : 2^+ \rightarrow 0^+)$  for the Sn isotopes from compilations [1], compared with some arbitrary parabolic shape and pseudo-SU3 results to be explained here (squares).

That these early results (Jonsson *et al.* [2]) truly signal a change of regime became evident through work on the unstable isomers, starting with the measure in  $^{108}\text{Sn}$  by Banu *et al.* [3]. A flurry of activity followed [4–10], from which a new trend emerged in which the parabola—characteristic of a seniority scheme—gives way to a platform, predicted by a pseudo SU3 scheme (the squares). Here we are going a bit fast to follow the injunction of Montaigne: start at the end (“Je veux qu’on commence par le dernier point” Essais II 10) [11, p. 298]. To slow

down, we go back to the origin of this study, the Cadmium isotopes, where quadrupole dominance is stronger and its consequences more clear-cut.

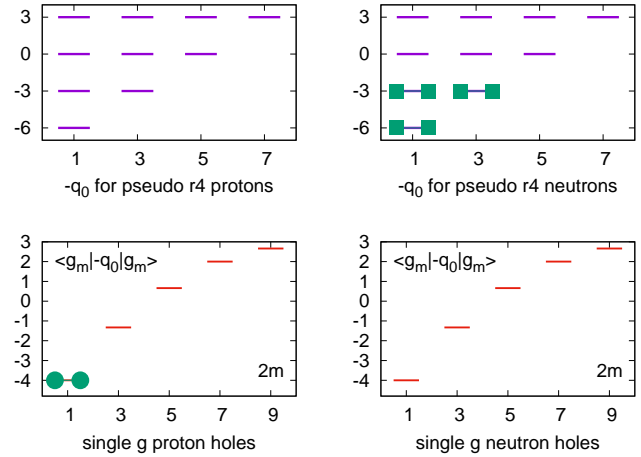


FIG. 2. The SP spaces adapted to the Cd and Sn isotopes. The (dimensionless)  $q_0 = \langle 2q_{20} \rangle$  values correspond to single particle and hole occupancies for the pseudo  $r_4$  and  $g$  cases respectively. The minus sign is an artifact to make occupancies start from the bottom. The figure illustrates the  $^{104}\text{Cd}$  configuration: circles for holes and squares for particles.

## I. THE CD ISOTOPES

The basic idea is inspired by Elliott’s SU3 scheme [12, 13] and consists in building intrinsic determinantal states that maximize  $q_0$ , the expectation value of the quadrupole operator  $\hat{q}_0 = 2q_{20}$ , *i.e.*,  $q_0 = \langle 2q_{20} \rangle$  [14–16]. Fig. 2 implements the idea for  $^{104}\text{Cd}$  ( $Z = 48$ ,  $N = 56$ ). The single shell (S) contribution of the  $g_{9/2} \equiv g$  proton orbit ( $Sg$ ) is given by Eq.(1) (with changed sign for hole states). For the neutron orbits, the pseudo SU3 scheme [16–18] (P generically,  $Pr_p$  for specific cases) amounts to assimilate all the orbits of a major oscillator shell of principal quantum number  $p$ , except the largest (the  $r_p$  set) to orbits in the  $p - 1$  major shell. In our case the  $sdg$  shell has  $p = 4$ , and  $r_4$  is assimilated to a  $pf$  shell. As

\* andres.zuker@in2p3.cnrs.fr

the  $\hat{q}_0$  operator is diagonal in the oscillator quanta representation, maximum  $\langle 2q_{20} \rangle$  is obtained by orderly filling states ( $n_z n_y n_x = (300), (210), (201) \dots (012), (003)$ ), with  $q_0 = \langle 2q_{20} \rangle = 2n_z - n_y - n_x = 6, 3, 3, 0, 0, \dots -3, -3$ , as in Fig. 2. Using  $q(n)$  for the cumulated  $q_0$  value (e.g. 24 for  $^{104}\text{Cd}$  in Fig. 2), the intrinsic quadrupole moment then follows as a sum of the single shell (S) and pseudo SU3 (P) contributions

$$q_0(S) = 2\langle r^2 C_{20} \rangle = \sum_m (p + 3/2) \frac{j(j+1) - 3m^2}{2j(j+1)} \quad (1)$$

$$q_0(P) = q(n), \quad Q_0(SP) = [(8e_\pi + q(n)e_\nu)b^2] \text{ efm}^2 \quad (2)$$

where we have introduced effective charges ( $e_\pi, e_\nu$ ) for protons and neutrons, and recovered dimensions through  $Q = b^2 q$  with

$$b^2 \approx 41.4/\hbar\omega \text{ fm}^2 \text{ and } \hbar\omega = 45A^{-1/3} - 25A^{-2/3}$$

To qualify as a Bohr Mottelson rotor,  $Q_0(SP)$  must coincide with the intrinsic spectroscopic  $Q_{0s}$  and transition  $Q_{0t}$  quadrupole moments, defined through (as, e.g. in Ref. [16])

$$Q_{spec}(J) = \langle JJ | 3z^2 - r^2 | JJ \rangle$$

$$Q_{0s} = \frac{(J+1)(2J+3)}{3K^2 - J(J+1)} Q_{spec}(J), \quad K \neq 1 \quad (3)$$

$$B(E2, J \rightarrow J-2) = \frac{5}{16\pi} e^2 |\langle JK20 | J-2, K \rangle|^2 Q_{0t}^2 \quad (4)$$

$$K \neq 1/2, 1, B(E2 : 2^+ \rightarrow 0^+) = Q_{0SP}^2 / 50.3 \text{ e}^2 \text{fm}^4 \quad (5)$$

To speak of deformed nuclei two conditions must be met:  $B(E2 : 4^+ \rightarrow 2^+)/B(E2 : 2^+ \rightarrow 0^+) = 1.43$  (the Alaga rule from Eq. (4)), and the ‘‘quadrupole quotient’’ rule,  $Q/q$  which follows from Eqs.(3) and (4) by equating  $Q_{0s} \approx Q_{0t}$ :

$$50.27B(E2 : 2^+ \rightarrow 0^+)/ (3.5Q_{spec})^2 = (Q/q)^2 \approx 1 \quad (6)$$

Full verification demands calculations but Eq. (5) can be checked directly by inspecting Fig. 2 as done in Table I.

Note that the naive form of P used so far (in  $q(n)_n$  and B20sp) is supplemented by the more accurate  $q(n)_f$  and B20SP using fully diagonalized values of  $\langle 2q_{20} \rangle$ . The remarkable property of the  $r_4^n$  space, that produces four identical  $q(n)_s$  values for  $m = 6 - 12$ , has already been put to good use in Ref. [14] and Ref. [15, Fig. 38, Table VII]. In the present case it is seen to do equally well.

Now for the shell model diagonalizations in spaces defined by  $(g^{X-u} r_4^u)_\pi (g^{10-t} r_4^{n+t})_\nu$ ,  $X = 8$  for Cd and 10 for Sn. The proton ( $u$ ) and neutron ( $t$ ) excitations are restricted to have  $u+t \leq M$ . The calculations were done for  $utM = 000$  (the case in Fig. 2), 111, 101 and 202 using  $V_{\text{low-}k}$  variants [21] of the precision interaction N3LO [22] (denoted as I in what follows) with oscillator parameter  $\hbar\omega = 8.4 \text{ MeV}$  and cutoff  $\lambda = 2 \text{ fm}^{-1}$ . As a first step the

TABLE I.  $B(E2 : 2^+ \rightarrow 0^+)$  estimates for  $^{98+n}\text{Cd}$  in  $\text{e}^2 \text{fm}^4$  from Eq.(5). B20sp uses naive  $q(n)_n$  from diagonalization of  $\hat{q}_0$  in the  $pf$  shell *i.e.*, strict SU3, with  $(e_\nu, e_\pi) = (1.1, 1.7)$ . The B20SP numbers use (full)  $q(n)_f$  from diagonalization of  $\hat{q}_0$  in the  $r_4$  space,  $(e_\nu, e_\pi) = (1.0, 1.5)$ . The  $b^2$  values range from  $4.78 \text{ fm}^2$  for  $A = 98$  to  $4.94 \text{ fm}^2$  for  $A = 110$ . Experimental values (B20e) for  $^{102-104}\text{Cd}$  are taken from [19] and [20], and from compilations [1] for  $^{106-110}\text{Cd}$ .

|          |         |         |         |         |         |         |
|----------|---------|---------|---------|---------|---------|---------|
| A        | 100     | 102     | 104     | 106     | 108     | 110     |
| n        | 2       | 4       | 6       | 8       | 10      | 12      |
| $q(n)_n$ | 12      | 18      | 24      | 24      | 24      | 24      |
| $q(n)_f$ | 14.8    | 22.6    | 29.5    | 30.0    | 29.6    | 29.3    |
| B20e     | <560(4) | 562(46) | 779(80) | 814(24) | 838(28) | 852(42) |
| B20sp    | 330     | 517     | 751     | 756     | 770     | 776     |
| B20SP    | 330     | 555     | 809     | 838     | 833     | 827     |

monopole part of I is removed and replaced by single-particle energies for  $^{100}\text{Sn}$  from Ref. [23] (referred to as GEMO for General Monopole: a successful description of particle and hole spectra on magic nuclei from Oxygen to Lead, in particular consistent with the analysis of Ref. [24] for  $^{100}\text{Sn}$ .)

The I interaction is then subject to an overall 1.1 scaling and renormalized by increasing the  $\lambda\mu = 20$  quadrupole and  $JT = 01$  pairing components by  $q \times 10\%$  and  $p \times 10\%$ , respectively. The resulting interactions are called I.q.p. According to Ref. [25] the quadrupole renormalization (due to  $2\hbar\omega$  perturbative couplings) amounts to 30%, a theoretically sound result, empirically validated by the best phenomenological interactions in the  $sd$  and  $pf$  shells. By the same token the effective charges in  $0\hbar\omega$  spaces are estimated as  $(e_\nu, e_\pi) = (0.46, 1.31)$ , as confirmed in Refs. [26, 27]. For the pairing component, perturbation theory is not a good guide, but comparison with the phenomenological interactions demands a 40% increase [15, 25]. It follows that I.3.4 and  $(e_\nu, e_\pi) = (0.46, 1.31)$  should be taken as standard for full  $0\hbar\omega$  spaces.

As we will be working in very truncated ones, renormalizations should be implemented. A hint comes from the need to reduce the very large effective charges invoked in Table I through polarization mechanisms that involve excitations to the  $g$  shell. Proton jumps will contribute to  $e_\nu$  and are expected to have greater impact than the corresponding neutron jumps, rapidly blocked by the  $(r_4^{n+t})_\nu$  particles. As a consequence we set  $e_\pi = 1.4$ , a guess close to the standard value, and let  $e_\nu$  vary, thus becoming the only adjustable parameter in the calculations. A choice validated later in section IV.

In Fig. 3 it is seen that  $utM = 000$  and 101 give the same results provided  $e_\nu$  is properly chosen. There is little difference between  $utM = 111$  and  $utM = 101$  because as soon as neutrons are added they block the corresponding jumps, as mentioned above.

The calculation yields near perfect agreement with the Alaga rule:  $(B(E2 : 4^+ \rightarrow 2^+)/B(E2 : 2^+ \rightarrow 0^+)) \approx 1.43B(E2 : 2^+ \rightarrow 0^+)$ . In the figure it is shown for  $utM = 101$  but it holds as well for 000 and 111. The

more stringent quadrupole quotient rule Eq. (6) yields an average  $Q/q = 0.96$  for  $^{106-110}\text{Cd}$ , corroborating the existence of a deformed region. A possibility anticipated in Ref. [28].

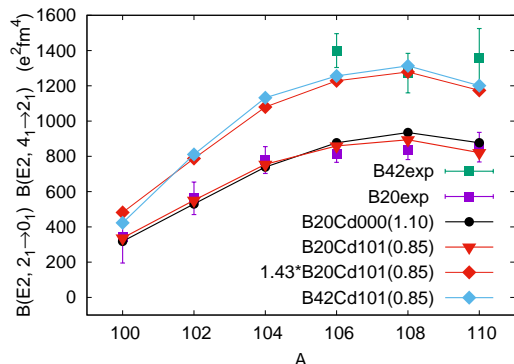


FIG. 3. . Experimental and calculated  $BE2$  rates for the Cd isotopes.  $B(E2 : 2^+ \rightarrow 0^+)$  values from from [19],[20], and [1].  $B(E2 : 4^+ \rightarrow 2^+)$  values from [29]. In parenthesis ( $e_\nu$ ),  $e_\pi = 1.40$  is fixed

## II. THE SN ISOTOPES

In moving to the tin isotopes the  $Pr_4$  part of the SP scheme becomes isolated and sensitive to details of the interaction. Bäck and coworkers [30, Fig. 3] suggest that a parabolic trend as found in Banu *et al.* [3], or schematically in Fig. 1, can be modified in a  $utM = 000$  context, by changes in the single-particle behavior, thus leading to the first tentative explanation of the plateau. The more complete calculations of Togashi *et al.* [31, Fig. 2] demand  $g$  excitations to achieve a satisfactory result, very close to ours in the upper Fig. 4, in spite of huge differences in the  $g$  proton occupancies (spin and mass dependent in their case and nearly constant in ours). No  $B(E2 : 4^+ \rightarrow 2^+)$  results are proposed in this reference.

### A. The $B(E2 : 4^+ \rightarrow 2^+)/B(E2 : 2^+ \rightarrow 0^+)$ anomaly and the pairing-quadrupole interplay

The basic tenet of this paper is that quadrupole dominance is responsible for the  $B(E2 : 2^+ \rightarrow 0^+)$  patterns in the light Cd and Sn isotopes. Which means that they should exhibit a pseudo SU3 symmetry. Hence, we expect the existence of an intrinsic state, implying the validity of the Alaga rule (defined after Eq. (4)). The expectation is fulfilled in Cd (Fig. 3) but it fails in Sn, as seen in Fig. 4. Let us examine what to make of it.

The  $B(E2 : 2^+ \rightarrow 0^+)$  rates are consistent with pseudo SU3 validity, and are immune to details. The  $B(E2 : 4^+ \rightarrow 2^+)$  rates are sensitive to the single-particle field and to the pairing strength

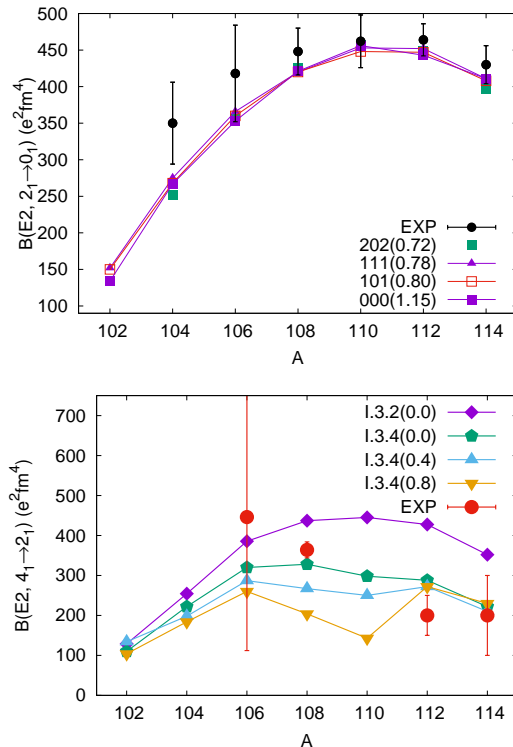


FIG. 4. .Upper panel: Experimental and calculated  $B(E2 : 2^+ \rightarrow 0^+)$  values for the Sn isotopes. I.3.4 interaction. In parenthesis ( $e_\nu$ ),  $e_\pi = 1.40$  is fixed. Experimental values from Ref [1]. Lower panel  $B(E2 : 4^+ \rightarrow 2^+)$  data from Jonsson *et al.* [2] for  $^{112-114}\text{Sn}$ , and from Siciliano *et al.* [32] for  $^{106-108}\text{Sn}$ . I.3.2( $\delta$ ) and I.3.4( $\delta$ ) calculations with the  $s_{1/2}$  single-particle energy displaced by  $\delta = 0.0, 0.4$  and  $0.8$  MeV with respect to the GEMO value of  $0.8$  MeV.

To test the influence of the single particle field on  $B(E2 : 4^+ \rightarrow 2^+)$  rates, the energy of the  $s_{1/2}$  orbit in  $^{101}\text{Sn}$  was displaced by  $0.0, 0.4$  and  $0.8$  MeV with respect to the present GEMO choice [23], called DZ (Dufo Zaker) in Ref. [24, Fig. 3.2.1] where an extrapolated value (EX) is given as reference. The position of the  $s_{1/2}$  orbit for DZ and EX differ by  $800$  keV. In the calculations reported In Fig. 4, I.3.4(0,0) and I.3.4(0,8) correspond to DZ and EX respectively. The  $B(E2 : 4^+ \rightarrow 2^+)$  differences are significant. Thanks to the recent  $^{108}\text{Sn}$   $B(E2 : 4^+ \rightarrow 2^+)$  measure of Siciliano *et al.* [32, Fig. 3b], the DZ choice is clearly favored.

The  $B(E2 : 4^+ \rightarrow 2^+)/B(E2 : 2^+ \rightarrow 0^+) < 1$  anomaly had been detected in  $^{114}\text{Xe}$  [33], in  $^{114}\text{Te}$  [34], and more recently in  $^{172}\text{Pt}$ , Ref. [35], where it is stressed that no theoretical explanation is available. Here, the sensitivity to the pairing strength provides a clue. In Fig. 4, its decrease in going from I.3.4 to I.3.2 produces a substantial increase of  $B(E2 : 4^+ \rightarrow 2^+)$ . As can be gathered from Ref. [32, Figs. 3a and 3b],  $B(E2 : 2^+ \rightarrow 0^+)$  is totally immune to pairing, while  $B(E2 : 4^+ \rightarrow 2^+)$  is so sensitive that a sufficient decrease in strength could bring

$B(E2 : 4^+ \rightarrow 2^+)/B(E2 : 2^+ \rightarrow 0^+)$  close to the Alaga rule. It appears that pairing is eroding the deformed band. Only the lowest  $J = 0$  and 2 are spared, giving way to a pairing-quadrupole interplay, that will eventually end up in pairing dominance at  $N \approx 70$ . Next we examine how the transition may take place.

### III. CD AND SN AT $N \geq 64$

In Table II the naive  $Pr_4$  adimensional intrinsic quadrupole moments for prolate (q0p) and oblate (q0o) are compared for Sn. The former are the same as  $q(n)_n$  in Table I. The latter are obtained by filling the platforms in reverse order (from the top). Up to  $N = 56$  prolate dominates. From  $N = 58$  to 62 there is oblate-prolate degeneracy. At  $N = 64$ , oblate dominates. The trend in sign indicated by the intrinsic values is respected by the calculated spectroscopic moments that opt for “oblate” shapes for  $N > 58$  *i.e.*,  $A > 108$ . For  $^{112-114}\text{Sn}$  the shell model results are close—for the quadrupole moments—or agree—for the magnetic moments—with the measured values. Note: The magnetic moments are very sensitive to the anomalous  $g_{l\nu}$  taken from Ref. [36].

TABLE II. Intrinsic adimensional q0 for prolate (q0p), and oblate (-q0o) states. Calculated spectroscopic quadrupole moments and g-factor, Q2, Q4, g for I.3.4 ( $e_\nu, e_\pi$ ) = 0.72, 1.40;  $g_{s\nu} = -2.869$ ,  $g_{l\nu} = -0.070$  [36],  $g_{s\pi} = 4.189$ ,  $g_{l\pi} = 1.100$ . Experimental Q2\* and g\* from Allmond *et al.* [37],  $g_{s\nu\pi}$  quenched by 0.75 with respect to the bare values [15, Fig. 28]

| N  | q0p | -q0o | Q2  | Q4  | Q2*  | g*        | g      |
|----|-----|------|-----|-----|------|-----------|--------|
| 52 | 12  | 6    | -18 | -24 |      |           | -0.157 |
| 54 | 18  | 12   | -21 | -21 |      |           | 0.012  |
| 56 | 24  | 18   | -16 | -17 |      |           | 0.103  |
| 58 | 24  | 24   | -5  | -02 |      |           | 0.142  |
| 60 | 24  | 24   | 3   | 10  |      |           | 0.142  |
| 62 | 24  | 24   | 14  | 26  | 4(9) | 0.150(43) | 0.135  |
| 64 | 18  | 24   | 25  | 43  | 9(8) | 0.138(63) | 0.106  |

So far the  $sdg$  space has proven sufficient as the effects of the  $h_{11/2}$  orbit ( $h$  for short) remain perturbative. For Sn we know from classic ( $p, d$ ) work [38], that the  $h$  occupancy—very small up to  $^{110}\text{Sn}$ —increases at  $^{112-114}\text{Sn}$ , as borne out by calculations that indicate the need of a boost of some 10% in  $B(E2 : 2^+ \rightarrow 0^+)$  [39] with respect to Fig. 4. Beyond  $N = 64$ , the explicit inclusion of the  $h$  orbit becomes imperative but the situation is different for the two families, as can be gathered in the transitional nuclei  $^{112}\text{Cd}$  and  $^{116}\text{Sn}$ .

For Cadmium the calculations give systematically prolate values in line with Stone’s Q tables [40], but in  $^{112}\text{Cd}$  (excluded from both Table I and Fig. 3) they yield severe underestimates whose correction necessitates the introduction of a quasi-SU3 mechanism (referred generically as Q in what follows, and  $Qhfh$  for the case we introduce next).

It is illustrated in Fig. 5, which will serve as a basis

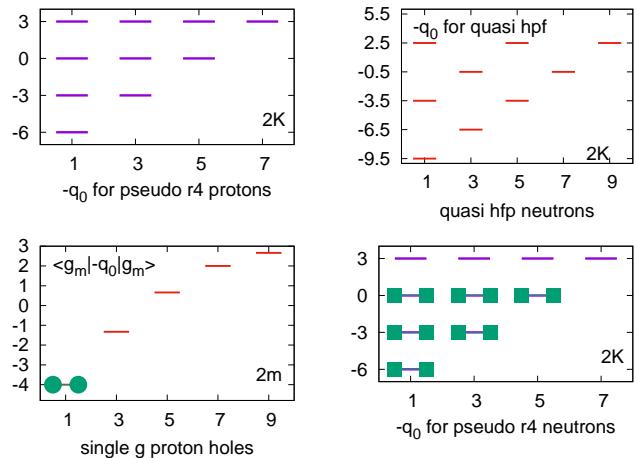


FIG. 5. The  $^{110}\text{Cd}$  intrinsic state in the SPQ space. The few lowest quasi SU3 ( $Qhfp$ )  $q_0$  platforms are obtained by diagonalizing the quadrupole operator  $\hat{q}_0$  in the  $hfp$  space *i.e.*, the degenerate  $\Delta J = 2$  sequence in  $pfh$  shell:  $h_{11/2}, f_{7/2}, p_{3/2}$ . A more realistic estimate must account for the splittings between the orbits which involves solving selfconsistently Eq (8) as explained in the text. The lowest resulting platforms are at  $\langle 2q_{20} \rangle = 5.0, 5.0$  (both  $k = 1/2$ ) and 4.0 ( $k = 3/2$ ).

to explore possible  $B(E2 : 2^+ \rightarrow 0^+)$ . Starting from Eqs.(2,5), adapted to  $^{110+k}\text{Cd}$  (or  $^{114+k}\text{Sn}$ , dropping the  $8e_\pi$  term)

$$B(E2 : 2_1 \rightarrow 0_1) = [8e_\pi + (24 + \zeta)e_\nu b^2]^2 / 50.3 \quad (7)$$

in  $\text{e}^2\text{fm}^4$ , which, using values from Table I,  $e_\nu = 1.1$  and  $b^2 = 5$ , yields  $B(E2 : 2^+ \rightarrow 0^+) = 800\text{e}^2\text{fm}^4$  (use round numbers in all that follows) for  $\zeta = 0$ , *i.e.*,  $^{110}\text{Cd}$ .

For  $^{112}\text{Cd}$  adding a  $Pr_4$  pair ( $\zeta = -6$ ) yields  $600\text{e}^2\text{fm}^4$ , too small against the observed  $1000\text{e}^2\text{fm}^4$ . The alternative is to promote one or two  $Qhfp$  pairs. As the  $q_0$  platforms in the figure are obtained under the assumption of single-particle degeneracy they yield huge rates ( $\zeta = 19$  or 32) for a total 1800 and  $2800\text{e}^2\text{fm}^4$  respectively. A more realistic estimate demands that  $q_0$  be evaluated in the presence of a single-particle field.

To do so examine [16, Eq.(19)] (remember  $q_0 = \langle 2q_{20} \rangle$ )

$$H = H_{sp} - \frac{\hbar\omega\delta}{3}\hat{q}_0 \equiv H_{sp} - \beta\hbar\omega\kappa\frac{\hat{q}_0}{\mathcal{N}^2}q_0 \quad (8)$$

$$\mathcal{N}^2 = \sum (2q_{20rs})^2 = \sum_{k=0}^p (k+1)(2p-3k)^2. \quad (9)$$

Eq. (8) compares the classic Nilsson problem to the left and the selfconsistent version to the right, which demands the solution of a linearized  $\hat{q}_0\hat{q}_0$  problem, subject to the condition that input and output  $q_0$  coincide. Hence,  $q_0$  the quantity we are after, is calculated while in the Nilsson case it is simply the parameter  $\delta$ . To have

all quantities entering the calculation fully defined, the norm of the  $\hat{q}_0\hat{q}_0$  Hamiltonian [16, Eq.(12)] is included:  $\mathcal{N}^2=420$  for  $p=5$ .

Written in full, the  $q_0$  part of  $H$  involves the  $S, P, Q$  cumulated pair contributions (the former from Eqs.(1,2)). Upon linearization, the factor  $\beta$  ensures that the single  $q_0 = q_0(Q)/2$  couples to the full  $q_0$ , and not only to itself, *i.e.*,  $\beta\langle q_0(Q)/2 \rangle = \langle (q_0(S)/2 + q_0(P)/2 + q_0(Q)/2) \rangle$ . Then  $\beta = 5$ , since  $q_0(S)/2 = 4$ ,  $q_0(P)/2 = 12$  and  $\langle q_0 \rangle \equiv q_0(Q) = 5.0$ .

The single-particle energies are taken from GEMO [23]  $\epsilon(h_{11/2}) = 0$ ,  $\epsilon(f_{7/2}) = 2.0$ ,  $\epsilon(p_{3/2}) = 3.0$  MeV

Recapitulating.  $\hbar\omega=8.34$ ,  $\kappa=0.3$  (the same as in the I.3.x interactions),  $\beta=5$ ,  $\mathcal{N}^2=420$ ,  $\langle q_0 \rangle = 5.0$ .

Then, solving for the right hand side of Eq. (8), leads to two  $k=1/2$  platforms at  $\langle 2q_{20} \rangle = 5$  and the  $k=3/2$  one at  $\langle 2q_{20} \rangle = 4$ , (as mentioned in Fig. 5). Combining them, the following values of  $\zeta = -6, 10, 18, 28$  lead, through Eq.(7), to  $B(E2 : 2^+ \rightarrow 0^+) = 600, 1300, 1800, 2500$   $e^2\text{fm}^4$  or, 19, 41, 56, 78 W.u. The first number is obtained by adding a  $Pr_4$  pair, the next three by adding 1, 2 and 3  $Qhfp$  pairs respectively. Note that for  $^{114}\text{Cd}$ , the promotion of two and three  $Qhfp$  pairs can be combined with one or two  $\langle 2q_{20} \rangle = 0$   $Pr_4$  holes. As a consequence the spectrum may contain bands for the four values above. Experimentally all these bands (and a couple more) are observed and fairly well reproduced by sophisticated beyond-mean-field calculations [41]. Here we only note that, experimentally, the ground state transition  $B(E2 : 2_1 \rightarrow 0_1) = 1000(100)$   $e^2\text{fm}^4$  or 31(3) W.u, compares with Rodríguez's [41] 38 W.u, and our 41 W.u, which may be somewhat reduced by increasing the  $hfp$  single-particle splittings.

It is seen that in the Cd family the full panoply of quadrupole agents **SPQR** (R for representations) is at play and can provide qualitative and some useful semi-quantitative results. Though only  $^{112}\text{Cd}$  has been examined, the context makes it clear that heavier isotopes will remain well deformed and that  $N=64$  signals a smooth merger between an  $SgPr_4$  scheme into a  $SgPr_4Qhfp$  one. That the heavier Cd isotopes are deformed was anticipated in Ref. [42].

In the case of Sn, the interaction favors oblate at  $N=64$  when it becomes the only option (consistent with data in Allmond *et al.*[37]). If we were to pursue the analogy with the Cd case we would expect the  $Pr_4$  scheme to merge into a  $Pr_4Sh$  one. According to Eq.(1) the lowest contributions  $-\langle 2q_{20} \rangle = 5, 2.27$  lead to  $\zeta = 10, 15$  and  $B(E2 : 2^+ \rightarrow 0^+) = 700, 900$   $e^2\text{fm}^4 = 22, 29$  W.u. Experimentally  $B(E2 : 2^+ \rightarrow 0^+) = 400$   $e^2\text{fm}^4 = 12$  W.u, too small, but there is a  $B(E2 : 0_2 \rightarrow 2_1) \approx 18$  W.u (in both  $^{116-118}\text{Sn}$ ), suggesting that the  $Pr_4Sh$  strength splits about equally with some intruder(s), as can be expected in a transition region. To go further, shell model calculations are called for. Though unmanageable for Cd, they are quite feasible in neutron only spaces throughout the Sn region. As they explain  $B(E2 : 2^+ \rightarrow 0^+)$  patterns in  $^{102-114}\text{Sn}$  and  $^{120-132}\text{Sn}$ , it is likely they will also do

so in  $^{116-120}\text{Sn}$  provided I.3.4 is adjusted to include the  $h_{11/2}$  orbit, and a more sophisticated monopole treatment of GEMO.

#### IV. THE INTERACTION AND THE MODEL SPACES

We have just mentioned the consequential result emerging from Fig. 4: the possibility to describe the  $B(E2 : 2^+ \rightarrow 0^+)$  pattern through a neutron-only calculation (the 000 case). This is at variance with previous calculations [3, 6, 30] using the CDB (Charge Dependent Bonn) potential [43], renormalized following Ref. [44]. Which raises two questions: why our I.3.x interactions succeeds where others fail? and why the neutron-only description is viable? They can answered simultaneously and we start by explaining how severely truncated spaces may represent the exact results, by comparing the largest calculation available with smaller ones. In Reference [32], results are given for  $^{106-108}\text{Sn}$  in  $utM = 444$  ( $m$ -dimensions  $10^{10}$ ) using the same interaction (called B in what follows) as in Banu *et al.* [3] (but omitting the  $h_{11/2}$  orbit). In Fig. 6 it is shown as B444 (circles) and

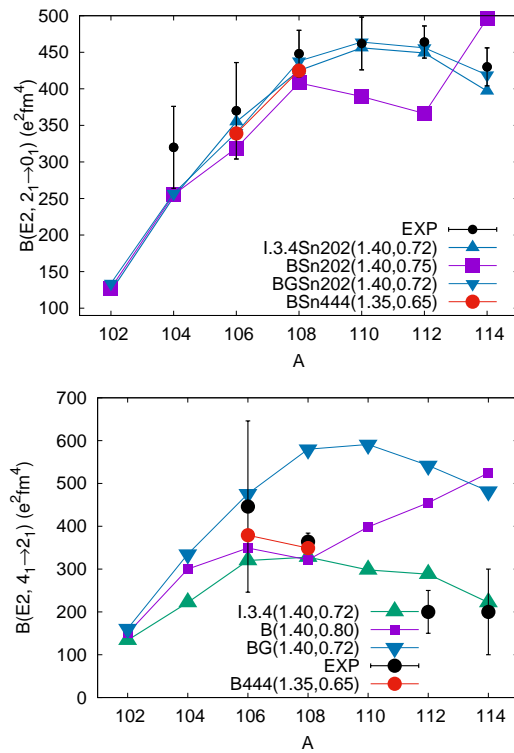


FIG. 6. Comparing calculations for B and I.3.4 interactions in the Sn isotopes. In parenthesis  $(e_\pi, e_\nu)$ . Experimental data as in Fig. 4. See text

compared with B202 (squares, the same interaction in our standard space). The agreement is very good for the

two points in  $B(E2 : 2^+ \rightarrow 0^+)$  and  $B(E2 : 4^+ \rightarrow 2^+)$ . The result amounts to a splendid vindication of the shell model viewed as the possibility to describe in a small space the behavior of a large one. Although in general the reduction from large to small spaces demands renormalization of the operators involved, for our purpose only the effective charges are affected. A non trivial fact that invites further study.

For much of the region, discrepancies between I.3.4 and B can be traced to poor monopole behavior of the latter. If the interaction is made monopole free and supplemented by the GEMO single-particle field used in our I.p.q forces, the resulting BG202 in Fig. 6 produces  $B(E2 : 2^+ \rightarrow 0^+)$  patterns identical to the ones for I.3.4-202, while for  $B(E2 : 4^+ \rightarrow 2^+)/B(E2 : 2^+ \rightarrow 0^+)$  the pattern is close to I.3.0 which is not shown, but can be guessed by extrapolation in Fig. 4 and from the analysis in Ref. [25] revealing the same  $q \cdot q$  content in I.3.4 and B, and a much weaker pairing for the latter; so weak in fact, that the B results come close to the Alaga rule.

It follows that for I.3.0, say, the  $Pr_4$  symmetry will hold, at least partially. As the pairing force is switched on, the  $J = 0_1, 2_1$  states are not affected, while  $J = 4_1$  is. Which points to an unusual form of interplay between the two coupling schemes—pairing and quadrupole—

traditionally associated to collectivity. In single fluid species, such as Sn, the seniority scheme can operate fully. It breaks down in the presence of two kind of particles, which turns to be the condition for quadrupole to operate successfully, as indicated by the Cd isotopes. What is unusual is the presence of quadrupole coherence in the light tins. It is shaky and challenged by pairing and we know that at about  $A = 120$  the seniority scheme will prevail. For the transition nuclei  $^{116-118}\text{Sn}$ , mixing of spherical and weakly oblate states is expected. Neutron-only calculations—in which the monopole field will play a crucial role—are likely to shed light on these matters.

The Sn isotopes were an example of pairing, then of quadrupole, then of pairing again. The world is but a perennial swing (Le monde n'est qu'une branloire perenne. Essais III 2 [11, p. 584]).

## ACKNOWLEDGMENTS

Alfredo Poves and Frédéric Nowacki took an active interest in the paper and made important suggestions. The collaboration with Marco Siciliano, Alain Goaduff and José Javier Valiente Dobón is gratefully acknowledged.

- 
- [1] B. Pritychenko, M. Birch, B. Singh, and M. Horoi, Tables of {E2} transition probabilities from the first states in even-even nuclei, *Atomic Data and Nuclear Data Tables* **107**, 1 (2016).
- [2] N.-G. Jonsson, A. Bcklin, J. Kantele, R. Julin, M. Luontama, and A. Passoja, Collective states in even sn nuclei, *Nuclear Physics A* **371**, 333 (1981).
- [3] A. Banu, J. Gerl, C. Fahlander, M. Górska, H. Grawe, T. R. Saito, H.-J. Wollersheim, E. Caurier, T. Engeland, A. Gniady, M. Hjorth-Jensen, and F. Nowacki,  $^{108}\text{Sn}$ , *Phys. Rev. C* **72**, 061305 (2005).
- [4] C. Vaman *et al.*,  $z = 50$  shell gap near  $^{100}\text{sn}$  from intermediate-energy coulomb excitations in even-mass  $^{106-112}\text{sn}$  isotopes, *Physical Review Letters* **99**, 162501 (2007).
- [5] J. Cederkäll, A. Ekström, C. Fahlander, A. Hurst, M. Hjorth-Jensen, *et al.*, Sub-barrier coulomb excitation of  $^{110}\text{sn}$  and its implications for the  $^{100}\text{sn}$  shell closure, *Physical Review Letters* **98**, 172501 (2007).
- [6] A. Ekström, J. Cederkäll, C. Fahlander, M. Hjorth-Jensen, *et al.*,  $0_{gs}^+ \rightarrow 2_1^+$  transition strengths in  $^{106}\text{sn}$  and  $^{108}\text{sn}$ , *Physical Review Letters* **101**, 012502 (2008).
- [7] R. Kumar, P. Doornenbal, A. Jhingan, R. K. Bhowmik, S. Muralithar, *et al.*, Enhanced  $0_{g.s.}^+ \rightarrow 2_1^+$  e2 transition strength in  $^{112}\text{sn}$ , *Physical Review C* **81**, 024306 (2010).
- [8] V. M. Bader, A. Gade, D. Weisshaar, *et al.*, Quadrupole collectivity in neutron-deficient sn nuclei:  $^{104}\text{sn}$  and the role of proton excitations, *Physical Review C* **88**, 051301 (2013).
- [9] P. Doornenbal, S. Takeuchi, N. Aoi, M. Matsushita, A. Obertelli, D. Steppenbeck, H. Wang, *et al.*, Intermediate-energy coulomb excitation of  $^{104}\text{sn}$ : moderate e2 strength decrease approaching  $^{100}\text{sn}$ , *Physical Review C* **90**, 061302 (2014).
- [10] R. Kumar, M. Saxena, P. Doornenbal, A. Jhingan, *et al.*, No evidence of reduced collectivity in coulomb-excited sn isotopes, *Physical Review C* **96**, 054318 (2017).
- [11] M.-L. Demonet, A. Legros, M. Duboc, L. Bertrand, and A. Lavrentiev, *Michel de Montaigne, Essais, 1588 (Exemplaire de Bordeaux), édition numérique générique (XML-TEI/ PDF)*, edited by M.-L. Demonet (2016).
- [12] J. P. Elliott, su3a, *Proc. Roy. Soc. London* **245**, 128 (1958).
- [13] J. P. Elliott, su3b, *Proc. Roy. Soc. London* **245**, 562 (1958).
- [14] A. P. Zuker, J. Retamosa, A. Poves, and E. Caurier, Spherical shell model description of rotational motion, *Phys. Rev. C* **52**, R1741 (1995).
- [15] E. Caurier, G. Martínez-Pinedo, F. Nowacki, A. Poves, and A. P. Zuker, The shell model as a unified view of nuclear structure, *Rev. Mod. Phys.* **77**, 427 (2005).
- [16] A. P. Zuker, A. Poves, F. Nowacki, and S. M. Lenzi, Nilsson-su3 self-consistency in heavy  $n = z$  nuclei, *Phys. Rev. C* **92**, 024320 (2015).
- [17] A. Arima, M. Harvey, and K. Shimuzi, *Phys. Lett. B* **30**, 517 (1969).
- [18] K. Hecht and A. Adler, Generalized seniority for favored j 0 pairs in mixed configurations, *Nuclear Physics A* **137**, 129 (1969).
- [19] A. Ekström, J. Cederkäll, D. D. DiJulio, C. Fahlander, and M. Hjorth-Jensen, Electric quadrupole moments of the  $2_1^+$  states in  $^{100,102,104}\text{Cd}$ , *Phys. Rev. C* **80**, 054302 (2009).
- [20] N. Boelaert, A. Dewald, C. Franssen, J. Jolie, A. Lin-

- nemann, B. Melon, O. Möller, N. Smirnova, and K. Heyde, Low-spin electromagnetic transition probabilities in  $^{102,104}\text{Cd}$ , *Phys. Rev. C* **75**, 054311 (2007).
- [21] S. Bogner, T. Kuo, and A. Schwenk, Model-independent low momentum nucleon interaction from phase shift equivalence, *Physics Reports* **386**, 1 (2003).
- [22] D. R. Entem and R. Machleidt, Accurate chiral potential, *Phys. Lett. B* **524**, 93 (2002).
- [23] J. Duflo and A. P. Zuker, The nuclear monopole hamiltonian, *Phys. Rev. C* **59**, R2347 (1999), program gemosp9.f in <https://www-nds.iaea.org/amdc/Duflo-Zuker...>
- [24] T. Faestermann, M. Górska, and H. Grawe, The structure of  $^{100}\text{Sn}$  and neighbouring nuclei, *Progress in Particle and Nuclear Physics* **69**, 85 (2013).
- [25] M. Dufour and A. P. Zuker, Realistic collective nuclear hamiltonian, *Phys. Rev. C* **54**, 1641 (1996).
- [26] H. L. Crawford, R. M. Clark, P. Fallon, and A. O. Macchiavelli, Quadrupole collectivity in neutron-rich Fe and Cr isotopes, *Phys. Rev. Lett.* **110**, 242701 (2013).
- [27] A. Blazhev, M. Górska, H. Grawe, J. Nyberg, M. Palacz, E. Caurier, O. Dorvaux, A. Gadea, and F. Nowacki, Observation of a core-excited  $e4$  isomer in  $^{98}\text{Cd}$ , *Phys. Rev. C* **69**, 064304 (2004).
- [28] T. Schmidt, K. L. G. Heyde, A. Blazhev, and J. Jolie, Shell-model-based deformation analysis of light cadmium isotopes, *Phys. Rev. C* **96**, 014302 (2017).
- [29] ANDT 107,1 (2016), <https://www.nndc.bnl.gov/nudat2>.
- [30] T. Bäck, C. Qi, B. Cederwall, R. Liotta, F. Ghazi Moradi, A. Johnson, R. Wyss, and R. Wadsworth, Transition probabilities near  $^{100}\text{Sn}$  and the stability of the  $n, z = 50$  shell closure, *Phys. Rev. C* **87**, 031306 (2013).
- [31] T. Togashi, Y. Tsunoda, T. Otsuka, N. Shimizu, and M. Honma, Novel shape evolution in Sn isotopes from magic numbers 50 to 82, *Phys. Rev. Lett.* **121**, 062501 (2018).
- [32] M. Siciliano and collaborators., (2019), pairing-quadrupole interplay in the neutron-deficient tin nuclei: first lifetime measurements of low-lying states in  $^{106,108}$ , arXiv:1905.10313v2, to appear in PLB.
- [33] G. de Angelis, A. Gadea, E. Farnea, R. Isocrate, P. Petkov, N. Marginean, D. Napoli, A. Dewald, *et al.*, Coherent proton-neutron contribution to octupole correlations in the neutron-deficient  $^{114}\text{Xe}$  nucleus, *Physics Letters B* **535**, 93 (2002).
- [34] O. Möller, N. Warr, J. Jolie, A. Dewald, A. Fitzler, A. Linnemann, K. O. Zell, P. E. Garrett, and S. W. Yates, E2 transition probabilities in  $^{114}\text{Te}$ : A conundrum, *Physical Review C* **71**, 064324 (2005).
- [35] B. Cederwall, M. Doncel, O. Aktas, A. Ertoprak, R. Liotta, C. Qi, T. Grahn, D. M. Cullen, B. S. Nara Singh, D. Hodge, M. Giles, and S. Stolze, Lifetime measurements of excited states in  $^{172}\text{Pt}$  and the variation of quadrupole transition strength with angular momentum, *Phys. Rev. Lett.* **121**, 022502 (2018).
- [36] R. Beck, R. Eder, E. Hagn, and E. Zech, Measurement of the anomalous neutron orbital  $g$  factor in  $^{190m}\text{Os}$ , *Phys. Rev. Lett.* **59**, 2923 (1987).
- [37] J. M. Allmond, A. E. Stuchbery, A. Galindo-Uribarri, E. Padilla-Rodal, and D. Radford, Investigation into the semimagic nature of the tin isotopes through electromagnetic moments, *Phys. Rev. C* **92**, 041303 (2015).
- [38] P. Cavanagh, C. Coleman, A. Hardacre, G. Gard, and J. Turner, A study of the nuclear structure of the odd tin isotopes by means of the (p, d) reaction, *Nuclear Physics A* **141**, 97 (1970).
- [39] F. Nowacki, Sn calculations in *sdgh* neutron spaces, private communication (2019).
- [40] N. Stone, Table of nuclear electric quadrupole moments, *Atomic Data and Nuclear Data Tables* **111-112**, 1 (2016).
- [41] P. E. Garrett, T. R. Rodríguez, A. D. Varela, K. L. Green, J. Bangay, A. Finlay, and *et al.*, Multiple shape coexistence in  $^{110,112}\text{Cd}$ , *Phys. Rev. Lett.* **123**, 142502 (2019).
- [42] T. R. Rodríguez, J. L. Egido, and A. Jungclaus, On the origin of the anomalous behaviour of excitation energies in the neutron-rich Cd isotopes, *Physics Letters B* **668**, 410 (2008).
- [43] R. Machleidt, F. Sammaruca, and Y. Song, Cd bonn, *Phys. Rev. C* **53**, R1483 (1996).
- [44] M. Hjorth-Jensen, T. T. S. Kuo, and E. Osnes, Realistic effective interactions for nuclear systems, *Phys. Rept.* **261**, 126 (1995).